Evaluation of Friction in the Chip-Tool Contact Interface

Fábio A. S. Baptista
fabio.baptista@tecnico.ulisboa.pt
Instituto Superior Técnico, Universidade de Lisboa, Portugal
September 2021

Abstract

Metal cutting processes involve friction mechanisms which are not fully understood. It's common to find on this subject literature values for the friction coefficient higher than the unit despite this being inconsistent with the mathematical theory of plasticity that governs the chip formation mechanism. The present work seeks to contribute to a better understanding of the metal cutting tribology through fundamental experimental research. The experimental development consisted on installing a test apparatus in order to perform tribological tests under controlled laboratory conditions. The test plan involved the evaluation of the friction coefficient for different cutting conditions on a large variety of materials under controlled atmosphere conditions. The use of restricted contact cutting tools (RT tools) allowed to assess the physical contribution of adhesion at the contact interface and to reveal the role of metallic oxidation regarding the friction mechanism.

Keywords:

Metal cutting processes, tribology, friction, adhesion, oxidation, orthogonal cutting.

1. Introduction

The frictional interaction at the chip-tool contact interface is not yet fully understood. Machining involves various physical and chemical phenomena which pose a challenge to its understanding and subsequent attempt to develop a theoretical model for the metal cutting process. Regarding the present work, a fundamental experimental investigation was carried out, focusing on the tribological analysis of the contact interface between the chip and the cutting tool, more specifically, the variation in the coefficient of friction with the use of inert and active gases. These gases, when interacting with the new chemically active metallic surfaces, may lead to the formation of oxides. The development of the experimental apparatus consisted in the installation of a test bench to carry out tribological tests under controlled laboratory conditions that are representative of the machining processes. The friction coefficient was estimated through the forces measured during the tests. Consequently, restricted contact tools were used for contact area control.

2. Theoretical Background

2.1. Asperities and Friction

The microscopic observation of any surface shows that it is not completely smooth, existing irregularities, generally called asperities, constituted by peaks and valleys (Fig.1). These surface characteristics are conditions that influence chip formation. In this way, they are linked to the finishing and protection of a machined part against corrosion and abrasion. The surface characteristics, temperature and atmosphere used in the

machining process also influence the slip of the chip on the tool's rake face. The tribology science usually uses the coefficient of friction to quantify the difficulty of slipping between materials. Friction is a phenomenon that results from several factors, namely two very important ones: adhesion and mechanical contributions (interlocking and plastic deformation) between surfaces.

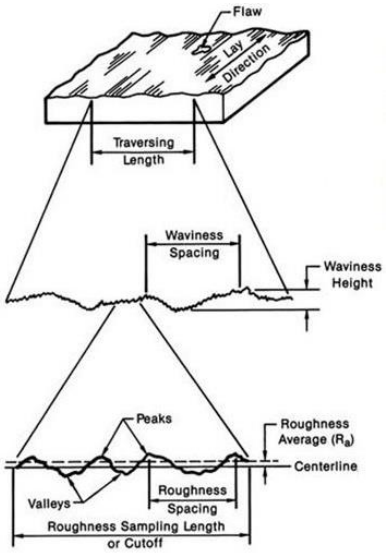

Figure 1 – Schematic representation of a real surface when analyzed at a microscopic level. (CENAM - División Metrología Dimensional)

2.2. Adhesion

Adhesion constitutes the connection between protuberances at an interface when subjected to high pressure, which can be called pressure welding and constitutes a bonding phenomenon that occurs at the atomic level. This phenomenon is extremely important in certain situations such as vacuum applications and cases where the surfaces are virgin or very clean. Adhesion is then implicit in the generation of friction. Regarding contact surfaces, according to Maugis (2001), if they are rough or contain impurities, adhesion is not expected to be relevant, and may not be verified at all. The absorption of impurities on the surfaces causes the metallic connections to be weakened, so that the adhesion decreases abruptly. Metallic surfaces without impurities have a high surface energy, which promotes stronger metallic bonds between them when there is contact. One example being metal cutting processes where there is contact between newly formed surfaces such as between the chip and the rake face of a cutting tool. According to Maugis and Barquins (1980), several experimental works demonstrated that immediately above a certain temperature, the adhesion between metals grows sharply with its continuous increase and contact time. It is considered as a representative value of this temperature approximately $0.3\,T_f$, being T_f the melting temperature of the respective metal. In conclusion, adhesion is an important factor in the study of friction in this work, since in addition to virgin surfaces on the specimen, the tool has its faces polished.

2.3. Friction Models

Taking into account the need to estimate the friction associated with different case studies, different friction models have been developed, thus, table 1 contains four of these models.

Table 1 – Friction Models.

Amontons-Coulomb	$\tau_f = \mu\sigma_n$	(1)
Prandtl Law	$\tau_f = m_f k$	(2)
Zorev	$\tau_f = \begin{cases} k, & 0 \le l \le l_p \\ \mu\sigma_n, & l_p \le l \le l_c \end{cases}$	(3)
Hybrid Model	$\tau_f = \begin{cases} m_f k, & 0 \le l \le l_p \\ \mu\sigma_n, & l_p \le l \le l_c \end{cases}$	(4)

The existence of different friction models is due to the fact that there are some limitations with the simpler models such as the Amontons-Coulomb model, which do not allow for a perfect modelling of the results obtained

in different fields of application. Thus, different authors have developed models that best apply to each field of application/research.

The Amontons-Coulomb theory, concerning the mechanics of contact between solid bodies, considers as the most relevant aspect that the coefficient of friction is independent of the real and apparent areas of contact, being uniquely and exclusively proportional to the applied forces and, consequently, to the stresses developed between the two surfaces. In the expression associated with this model, μ corresponds to the dimensionless friction coefficient, σ_n to the stress normal to the contact surface between the two bodies, τ_f to the resulting frictional shear stress.

Manufacturing processes such as machining that involve plastic deformation of metallic materials are characterized by having high contact pressures in the contact zone between the material and the tool. As such, to better analyse processes with high contact pressures the Prandtl model is often used. In this second model, m_f is called the friction factor and represents a correction of the material's shear yield stress, k. The m_f factor ranges from 0 to 1. In the Zorev model (fig. 2), it's possible to distinguish two regions: in the sticking region (l_p) we have the maximum friction situation described in the Prandtl model with the shear stress equal to the material's shear yield stress; in the sliding region ($l_p \leq l \leq l_c$), the friction behaviour can be modelled using the Amontons-Coulomb model. Regarding the hybrid model, the two previously mentioned regions are distinguished again, applying the Prandtl model in the first, in which the friction factor varies between 0 and 1. While the Amontons-Coulomb model is applied in the second.

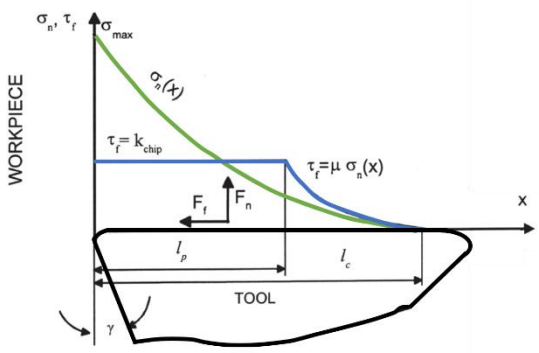

Figure 2 – Schematic representation of the normal and frictional shear stress distribution along the tool rake face. (Özel and Altan, 2000)

2.4. Orthogonal cutting

There are several methods that are used experimentally to study friction, such as the pin-on-disk test. The experimental work developed by Cristino (2007) showed that the influence of the surrounding environment on the friction coefficient can be analyzed by observing the chip formation in the orthogonal cut. Thus, in the case of the present work, for the analysis of friction, the orthogonal cutting test is also carried out.

On both the rake and clearance surfaces of the tool, friction plays an important role as there is contact between moving bodies. Thus, there is an interest in studying friction in the process in order to minimize it. Thus, the acquisition of data in the experimental test corresponds to the measurement of the cutting (F_n) and thrust (F_t) forces through a load cell. As the tools tested have a rake angle of zero, the horizontal and vertical forces measured directly by the load cell coincide respectively with the cutting and thrust forces (Eq. 5). The β parameter represents the friction angle.

$$\frac{F_t}{F_n} = \tan\beta = \mu \quad (5)$$

The chip formation process is very sensitive to the tribological conditions on the

rake face. For example, reducing the coefficient of friction leads to an increase in the cutting plane angle, ϕ, and a reduction in chip thickness, as well as an increase in chip curvature as shown in Fig. 3. A lower coefficient of friction also results in a smaller area of the cut plane, less pressure and contact length on the rake face, with the final consequence being a reduction in the resulting force needed to make the cut.

The formation of the chip is accompanied by the exposure of new surfaces. These surfaces are chemically very active and raise particular tribological conditions regarding adhesion, among others. The use of lubricant, be it solid, liquid or gas, in the cutting process, allows to vary the tribological conditions at the interface between the chip and the tool. In the present work, dry contact has been employed under controlled surrounding conditions.

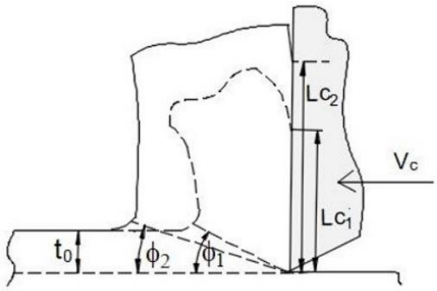

Figure 3 – Influence of friction conditions on contact length and chip curvature.

3. Development of Experimental Apparatus

3.1. Tribological Tests Machine

In order to perform the tribological tests, a CNC milling machine was adapted and used during the experimental work. This machine has 3 axes and a vertical spindle with the possibility of being controlled manually or via programming with G code. To carry out the tests, a device for fixing the specimen to be tested was designed (Fig. 4), as well as a device for fixing the grinding wheel (Fig. 5). The first device has a place for fitting circular specimens as well as a rectilinear step for larger rectangular specimens.

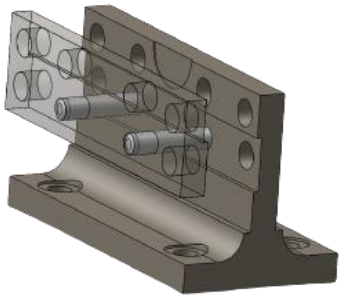

Figure 4 – Fixing device for specimens of orthogonal cutting tests.

After each cutting test there is a surface layer of material that undergoes work hardening, therefore the mechanical properties of the surface material change. In order to be able to carry out successive tests of orthogonal cutting on the same specimen with the material having the same properties in all tests, it is necessary to carry out a grinding operation that removes the mechanically affected layer with a grinding wheel. The grinding wheel is fixed to the spindle of the machine using a R8 taper with easy change holder (Fig. 5).

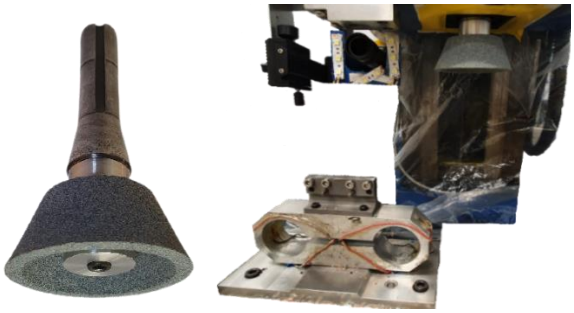

(a) (b)

Figure 5 – Various accessories of the experimental apparatus. (a) Grinding wheel and R8 holder; (b) Elements of the apparatus inside the atmospheric chamber.

The thickness of the hardened layer of material has been studied and it has been decided to remove a layer of material from the specimen with a thickness equal to the cutting thickness of the last test performed. The

grinding wheel used has a mesh of 80 particles per square inch. To register the experimental tests there is a camera (Fig. 6) which registers a film with the chip formation. The video camera has a support that allows adjustment in the Y and Z axes and the lens allows the adjustment of the focus. The orthogonal cutting tests were carried out in a controlled atmosphere using an active (oxygen) or inert (argon) gas, thus a flexible chamber has been mounted around the specimen and the cutting tool (Fig. 7). An assembly was carried out to ensure the proper sealing of the flexible chamber. To control the interior atmosphere, a flow meter connected to a cylinder with the desired gas is used. There is a system with a gas inlet control valve and quick-release pneumatic connectors.

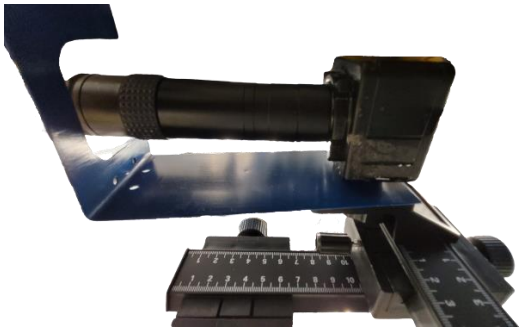

Figure 6 – Camera and the respective support.

Figure 7 – Tribological testing machine with the atmospheric chamber and gas cylinders.

To handle the specimens inside the atmospheric chamber without opening the casing and losing all the gas inside, creating unnecessary waste, there are two gloves that allow handling objects inside the chamber. A load cell was mounted on the testing machine's worktable. The load cell is composed of an aluminum block with strain gauges (Fig. 8(a)) that allow measuring the horizontal (cutting) and vertical (thrust) forces, and it should be noted that for a correct reading of the force values, the load must be applied in the center of the upper surface of the block, taking into account the shape of it. To measure the thickness of the material layer removed in each cut performed, a micrometer was used (Fig. 8(b)). For data acquisition, a DAQ board connected to a computer was used, using the Labview 8.5 software. This software registers the electrical voltage from the load cell strain gauges. However, the electrical signals emitted by the strain gauges are of a very small order of magnitude so there is a need for these signals to be processed by an intermediate unit, National Instruments USB-9162, which amplifies the voltage of the strain gauges and then communicates directly with the computer.

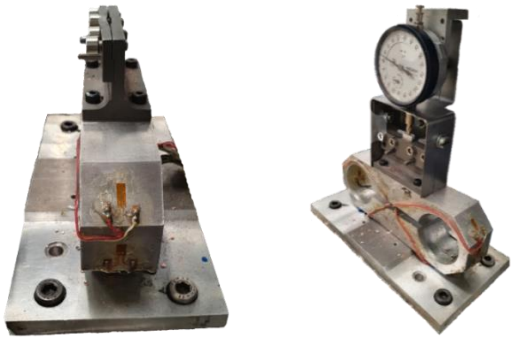

(a) (b)

Figure 8 – Load cell and specimen fixing device. (a) Extensometer on the side of the aluminum block; (b) Micrometer with comparator dial.

4. Cutting Tools Preparation

Orthogonal cutting tests were performed with restricted contact tools. Thus,

all cutting tools derived from the same base, from which processes were carried out (Fig. 9) to change the contact length on the rake face, the coating and its roughness (although in the present work only polished tools were tested except for the Palbit commercial tool).

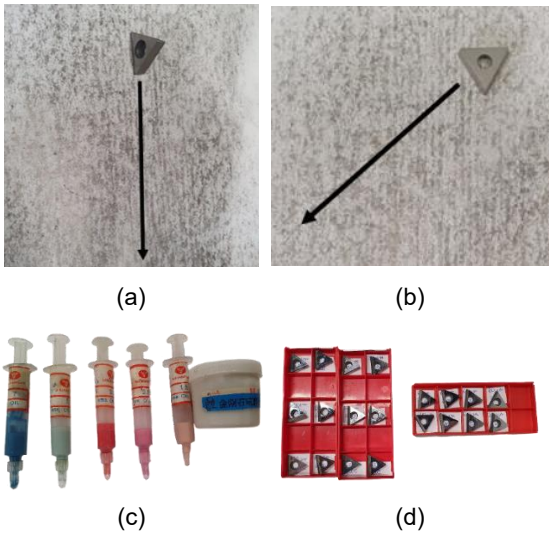

Figure 9 – Preparation procedure of the cutting tools. (a) Clearance face's direction of polishing; (b) Rake face's direction of polishing; (c) Different abrasive pastes; (d) Cutting inserts organized by roughness level.

From the twenty-two cutting tools available initially, groups of four were created, varying the contact length of the rake face in each group (30, 60, 120, 240 or 480 µm), plus the commercial and reference tools (RTØ). In each tool of the five groups mentioned, a notch was cut through a laser cutting process, obtaining a smaller effective rake face and consequently creating a chipbreaker (Fig. 10). The RT30, RT120 and RT480 sets of tools were coated using a Physical Vapor Deposition (PVD) process using High-Power Impulse Magnetron Sputtering (HiPIMS) technology, resulting in a 2.5 µm thick TiAlSiN coating.

5. Experimental Results

Orthogonal cutting tests were performed with a passage of the cutting tool on the specimen in a single direction, which were called unidirectional tests. A variation of this type of test was also carried out, in which the tool movement is stopped in the center of the specimen and then removed in an ascending movement of 90º with the initial movement direction. This second type of test was called bidirectional test (Fig. 12). These two types of tests present different behaviors in terms of the graphs of forces and friction coefficient.

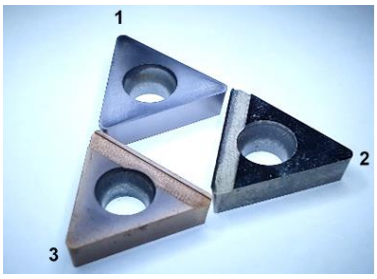

Figure 10 – Visual comparison between the different stages of preparation of a cutting tool: a commercial Palbit tool (1), a polished tool (2) and a polished and coated tool (3).

Unidirectional tests were carried out with material samples of AA1085 and pure copper as well as different types of cutting tools (Fig. 11) which reveal different levels of energy/force required under similar experimental conditions with controlled atmosphere. Fig. 11(a) shows the evolution of the cutting force with the depth of cut for the annealed copper. The cutting force increases linearly with thickness for all tested cutting conditions. However, it is possible to observe the existence of four distinct groups, parallel to each other and separated by a constant force value, for the different conditions of the cutting tool: (i) the commercial tool (without restricted contact and without polishing); (ii) the reference tool (non-restricted contact and polished without coating); (iii) with restricted contact and polished without coating; (iv) with restricted contact, polished and coated. The reference tool (RTØ) reveals higher values of the cutting force compared to the tools with restricted contact. Among the restricted contact

tools, those with a TiAlSiN coating present an increase in cutting force. This result seems to be related to their surface roughness. Fig.11(b) shows the evolution of the thrust force with the cut section. The analysis of these results indicates that they are at all similar to those previously described for the cutting force. In the Fig. 11(c) the evolution of the specific cutting pressure with cut thickness is visible. The graph clearly shows a decrease in the specific cutting pressure value with increasing cutting thickness. This evolution appears to be independent of the type of tool used and follows a model described by a negative exponent power function. From Fig. 11(d) it can be concluded that the four groups of tools present different trends in the relationship between the cutting and thrust forces, however, it is verified the existence of linearity within each of these four groups. The slope of the straight lines indicates that the level of friction is lower in the case of tests with uncoated tools and restricted contact, being the highest in tests with the commercial tool.

Taking into account that hundreds of tests were performed and it's not possible to present all the graphs (such as the forces and friction coefficient) for each test in this document, it was chosen to summarize the results regarding the friction coefficients of some tests in the following tables 2, 3 and 4. In tables 2 and 3 it is possible to compare the average friction coefficients obtained for the three most analysed materials. Their analysis reveals that similar results were obtained for equal conditions, with the most significant deviation being that referring to the bidirectional test of a copper specimen hardened with the RTΟΟ tool with a value of μ equal to 0.42 against the value of 0.32 obtained in the test equivalent unidirectional. From table 2, it can be seen that, in general, the commercial tool has higher friction coefficient values, followed by those of the RTΟΟ tool, then moving on to the average values of the group of coated tools RT30, RT120 and RT480, ending in the lower average values with the group consisting of RT60 and RT240 tools. The results in table 4 regarding the 18Ni 300 grade maraging steel and AISI 1045 show very similar values for both tools, obtaining even higher friction coefficient values for the RT480 tool than for RTΟΟ. However, for Ti the results indicate clearly lower μ values for RT480 than RTΟΟ. It is important to highlight that these results were obtained with an ambient atmosphere. Tests carried out with the RT480 tool reveal a lower friction coefficient at the chip and rake face interface than in the tests carried out with the reference tool (RTΟΟ), this trend being independent of the atmosphere used (ambient atmosphere or argon). This is consistent with what was expected, bearing in mind that this RT480 tool has a coating that allows for reduced adhesion against the reference tool. These results were obtained despite the RTΟΟ tool being polished and the RT480 having gone through a process of shot blasting prior to the application of its coating, which resulted in an increase in roughness making that tool no longer truly polished (the same happened for the RT30 and RT120 tools).

Table 2 – Friction coefficient (unidirectional tests).

Tool	AA1085 (Hardened)	Copper (Hardened)	Copper (Annealed)
RT30	0.58	0.33	0.34
RT120	0.52	0.41	0.28
RT480	0.58	0.31	0.22
RT60	0.51	0.35	0.24
RT240	0.44	0.27	0.25
RTΟΟ	0.62	0.32	0.32
Stock	0.71	-	0.38

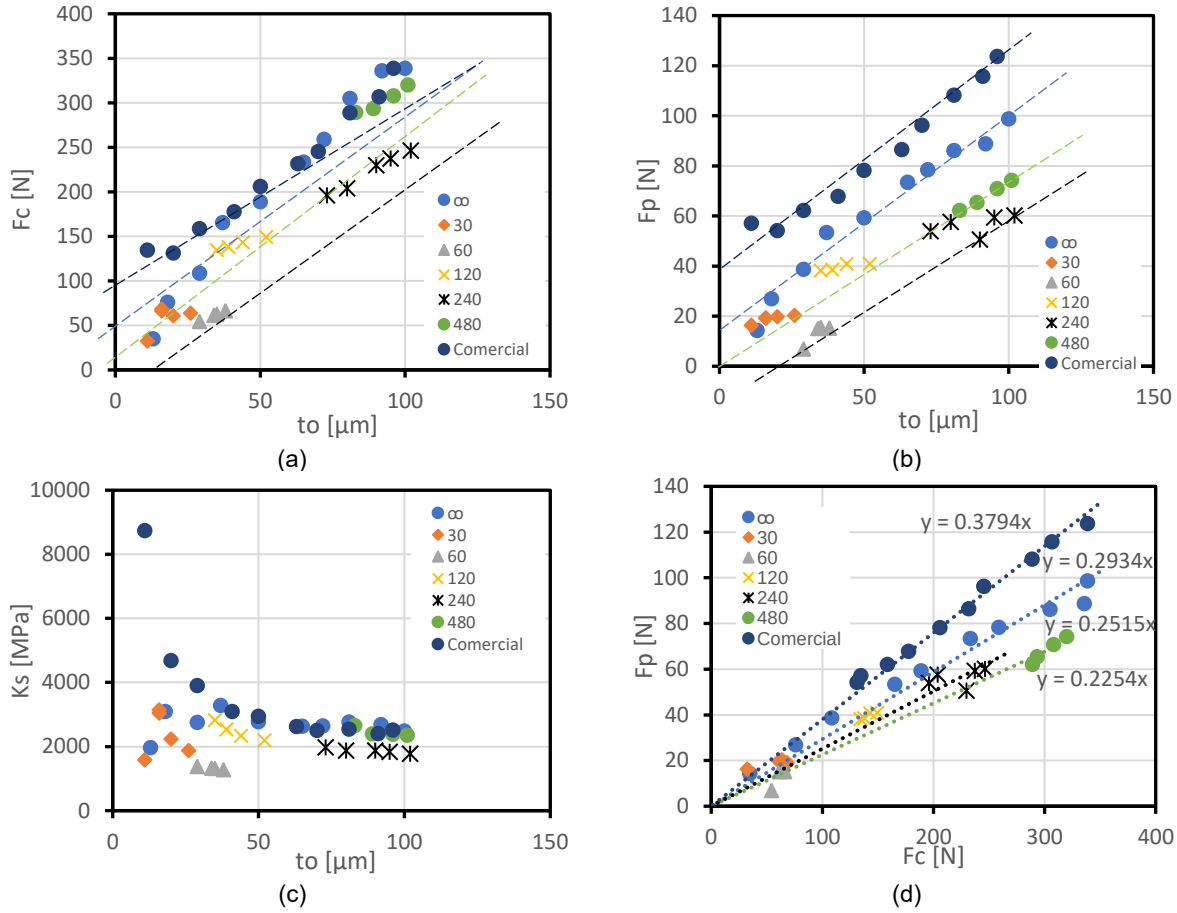

Figure 11 – Tests under orthogonal cutting condition (Copper (annealed), $V_c = 45\ mm/min$, $w_a = 1.36\ mm$, argon, Wc-Co, $R_a \approx 0.01\ \mu m$). (a) Evolution of cutting force with cutting thickness; (b) Evolution of thrust force with cutting thickness; (c) Evolution of specific cutting pressure with cutting thickness; (d) Relationship between cutting and thrust forces.

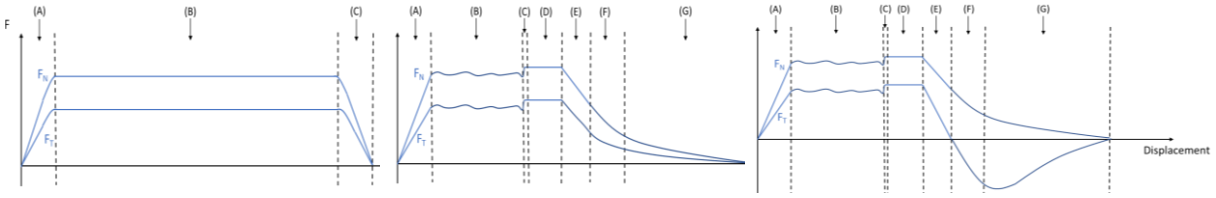

Figure 12 – Analysis of the different phases (A) to (G) of uni and bidirectional tests. (a) Graphic signature of a unidirectional test; (b) Graphic signature of a bidirectional test where the tangential force is always positive; (c) Bidirectional test with reversal of the tangential force direction.

Table 3 – Friction coefficient (bidirectional test).

Tool	Direction	AA1085 (Hardened)	Copper (Hardened)	Copper (Annealed)	Zinc (Hardened)
RT480	Horizontal	0.54	0.28	0.20	0.45
	Vertical	*			0.28
RT∞	Horizontal	0.62	0.42	0.33	0.73
	Vertical	*		0.12	0.30

* It wasn't possible to get a valid value from the graphs

6. Conclusions

Through an analysis of the experimental results, conclusions were drawn from them. This way, it becomes possible to improve the laboratory techniques used and, at an industrial level, the use of coated cutting tools and/or with restricted contact length on the rake face. The difficulties initially felt in

terms of the correct cutting depth to be tested for each tool and the reconditioning of them posed a challenge but the repetition of tests and the continuous improvement of the experimental procedure allowed to correct these points, obtaining thus valid experimental tests for the study carried out. The chip formation for tests carried out using tools with higher contact lengths (240 and 480 μm) didn't reach a steady state. This is reflected in the measured forces and in the results obtained therefrom potentially with significant deviations. Thus, in future works, material samples with a higher length should be used. The length and depth of the box on the rake face of the tools has an influence on the occurrence of chip collisions with the tool after the initial contact length. Thus, the opening of deeper notches and with greater length allows to validate more tests keeping the contact length constant. However, a negative consequence of the increase in these two parameters is the fact that the tool becomes less resistant to mechanical stresses in the lower zone close to the attack face, due to the smaller amount of material in that zone, which can lead to tool fracture. In conclusion, the commercial tool has the highest values of friction coefficient, followed by the reference tool and the coated tools group, ending up with the lowest values of the non-coated restricted contact tools. This hierarchy that has been established within the types of tools tested allows us to understand which tools generate energy savings by requiring less force during cutting and, therefore, less power to industrial equipment that uses these types of tools.

Table 4 – Friction coefficient (bidirectional tests, atmosphere).

Tool	Direction	18Ni 300 AMed	AISI 1045 (Hardened)	Ti (Hardened)
RT480	Horizontal	0.65	0.60	0.54
	Vertical	0.40	0.49	0.38
RTCO	Horizontal	0.62	0.61	0.73
	Vertical	0.25	0.48	0.66

References

CENAM, División Metrología Dimensional, Laboratorio de Acabado Superficial (2021, July 25). Retrieved from: https: //www.cenam.mx/ dimensional/laboratorios/acabadosuper.

Cristino V., Experimental Assessment of Analytical Solutions for Orthogonal Metal Cutting, Master Thesis, Instituto Superior Técnico, Lisboa, 2007.

Maugis, D., Barquins, M., Fracture mechanics and adherence of viscoelastic solids, in Adhesion and Adsorption of Polymers, Part A, Lee, L.H. (Ed.), Plenum Press, New York, p. 203, 1980.

Maugis D., Chapter 4 – Adhesion of Solids: Mechanical Aspects, Modern Tribology Handbook, Volume One, CRC Press LLC, Florida, 2001.

Özel T. e Altan T., Determination of workpiece flow stress and friction at the chip–tool contact for high-speed cutting. International Journal of Machine Tools and Manufacture, 40(1):133–152, 2000.

Zorev N. N., Inter-relationship between shear processes occurring along tool face and shear plane in metal cutting. International research in production engineering, 49:143–152, 1963.